Diverting photosynthetic electrons from suspensions of Chlamydomonas reinhardtii algae - New insights using an electrochemical well device

Adnan Sayegh, Guillaume Longatte, Olivier O. Buriez, Francis-André Wollman, Manon Guille-Collignon, Eric E. Labbé, Jérôme Delacotte, Frédéric Lemaître

Research Paper for Electrochimica Acta

Diverting Photosynthetic Electrons from Suspensions of *Chlamydomonas reinhardtii* Algae - New Insights using an Electrochemical Well Device

Adnan Sayegh,[a] Guillaume Longatte,[a] Olivier Buriez,[a] Francis-André Wollman,[b] Manon Guille-Collignon,[a] Eric Labbé,[a] Jérôme Delacotte,[a] Frédéric Lemaître[a]*

a) *PASTEUR, Département de Chimie, Ecole Normale Supérieure, PSL University, Sorbonne Université, CNRS, 75005 Paris, France.*

b) *Laboratory of Membrane and Molecular Physiology at IBPC, UMR 7141, CNRS/Sorbonne Université, 13 rue Pierre et Marie Curie, 75005 Paris, France*

Number of figures: 8

ABSTRACT

In the last years, many strategies have been developed to benefit from oxygenic photosynthesis in the present context of renewable energies. To achieve this, bioelectricity may be produced by using photosynthetic components involved in anodic or cathodic compartments. In this respect, harvesting photosynthetic electrons from living biological systems appears to be an encouraging approach. However it raises the question of the most suitable electrochemical device. In this work, we describe and analyze the performances of an electrochemical device based on a millimeter sized well involving a gold surface as a working electrode. Photocurrents were generated by suspensions of *Chlamydomonas reinhardtii* algae using quinones as mediators under different experimental conditions. Chronoamperometry and cyclic voltammetry measurements gave insight into the use of this device to investigate important issues (harvesting and poisoning by quinones, photoinactivation…). Furthermore, by introducing a kinetic model originally developed for homogeneous catalytic systems, the kinetics of the electron diverting from this system (*Chlamydomonas reinhardtii* algae + 2,6-DCBQ + miniaturized setup) can be estimated. All these results demonstrate that this experimental configuration is suitable for future works devoted to the choice of the best parameters in terms of long lasting performances.

Keywords: photosynthesis; quinones; electrochemistry; *Chlamydomonas reinhardtii* algae; photocurrent

1. Introduction

Producing electricity from natural photosynthesis is still a burgeoning field.[1] Photosynthesis is the process used by plants, cyanobacteria and algae to convert sunlight into chemical energy eventually stockpiled as carbohydrates. Briefly, light absorption by chlorophyll antenna induces excitation of the Photosystem II (PSII that transfers its energy to the PSII primary donor, P680 (chlorophyll dimers)). The subsequent charge separation results in water oxidation and in some electron transfer steps along the chain (plastoquinone (PQ) / plastoquinol (PQH_2) pool $\rightarrow$ cytochrome b_6f (b_6f) $\rightarrow$ plastocyanin (PC) $\rightarrow$ Photosystem I (PSI) $\rightarrow$ Ferredoxin (Fd) $\rightarrow$ Ferredoxin-$NADP^+$ reductase (FNR)) that lead to the $NADP^+$ reduction (**Figure 1A**). The consecutive ATP production by ATP synthase finally leads to CO_2 reduction by the mean of the Calvin cycle.

Taking advantage of natural photosynthesis generally occurs by using an outer polarized electrode for collecting a fraction of the electron flow along the photosynthetic chain. This harvesting strongly depends on the biological target, as summarized in several reviews.[2-4] In fact, using isolated photosystems (PSII and PSI) as photochemical converters is one of the best strategies to favor electron transfer between the photosynthetic target and the collecting electrode.[5-7] Nevertheless, it raises the question of the stability/denaturation of these systems outside their biological environment. This is why isolated thylakoid membranes or chloroplasts are also considered.[8-12] Yet, the lack of cell proliferation of these two strategies is an important issue and pushes toward the investigation of intact photosynthetic organisms.[13-17] However, the more complex the target is, the more difficult is the electron transport ways toward the electrode.[18] Indeed, direct harvesting from a photosynthetic organism is rather scarce.[19-21] This is why electron shuttles including soluble mediators (quinones, $Fe(CN)_6^{3-}$…), redox polymers and nano-objects are used as complementary tools to enhance photocurrent production.[2] Of course, the distance between the photosynthetic target and the electrode is another important issue that determines the experimental configuration (immobilization *vs*. suspension).

In this context, we have recently investigated an experimental configuration where a *Chlamydomonas reinhardtii* algae suspension was mixed with exogenous quinones.[22, 23] Living algae suspension was used because it potentially ensures its own culture and proliferation during the electron extraction process. To collect the photosynthetic electrons a polarized carbon gauze electrode (geometric surface ~1 cm^2) was used to oxidise hydroquinone (QH_2) on its surface.[24, 25] However, though performances in terms of

current magnitude (up to 60 µA cm^{-2}) were quite encouraging, quinones exhibited an antagonistic behaviour.[26] Indeed, quinones acted as good electron carriers but also as poisoning agents.[27] Chronoamperometry measurements helped in the identification of different poisoning pathways, but several issues are difficult to address with this set-up. On the one hand, the relatively large size of the carbon gauze electrode led to high equilibration times that required long timeframes (~1h) to be neglected before the proper experiment. On the other hand, it corresponded to quite large time constants that required long (and possibly photoinactivating) irradiation times to reach a steady state photocurrent. Furthermore, even though it is slightly less crucial, the preparative scale involved the use of forced convection conditions that are energy consuming. As a consequence, these main drawbacks prevent the use of this former set-up to achieve both systematic and comprehensive analyses of quinones. Because the role of quinones derivatives as photosynthetic electron cargos is still a matter of interest,[9, 13, 27, 28] we therefore report on a device aimed at decreasing the size of the photoelectrochemical cell. The use of a miniaturized well-type electrochemical device (**Figure 1B**) results in diminishing the experimental average time and allows exhaustive parameter analyses. Furthermore, the use of a mechanistic model originally devoted to classic homogeneous systems allows fast qualification of the performances of a given algae/mediator couple in a semi-quantitative way. Here the main properties of the generated photocurrents can thus be described and analyzed as a function of several experimental parameters in order to have in the future a better understanding of phenomena occurring in both algae and extracellular medium during electron harvesting.

2. Experimental

2.1.Cell culture and preparation

Chlamydomonas reinhardtii algae (wild-type or mutants) were grown in Tris Acetate Phosphate aqueous medium (TAP) containing Tris base (20 mmol L^{-1}), NH_4Cl (7 mmol L^{-1}), $MgSO_4$ (0.83 mmol L^{-1}), $CaCl_2$ (0.45 mmol L^{-1}), K_2HPO_4 (1.65 mmol L^{-1}), KH_2PO_4 (1.05 mmol L^{-1}), CH_3CO_2H (0.3 mmol L^{-1}) at 25°C under rather dim light conditions (50 µE m^{-2} s^{-1}) to a cell suspension at a concentration of 2.10^6 cells mL^{-1}, then centrifugated at 4000 rounds min^{-1} before being re-suspended into Tris-minimal medium (TAP without acetate) for electrochemical experiments (see below) to reach a final steady concentration of 2.10^7 cells mL^{-1} that corresponds to stable conditions for algae. In specific cases, Tris-minimal medium

supplemented with Ficoll 400 (10% w/w) was used and prepared according to the reference [29].

2.2. Chemical materials and solutions preparation

All chemicals including quinones have been purchased from sigma Aldrich and have been used without any further purification. In this work, 2,6-dichlorobenzoquinone (2,6-DCBQ) and 2,6-dimethylbenzoquinone (2,6-DMBQ) were selected owing to their different ability to harvest photosynthetic electrons from algae.[22, 24] Practically, quinones were dissolved in absolute ethanol in order to make mother solutions (10 mmol L^{-1}). Appropriate small volumes of these solutions were thus directly added to the algae suspension for subsequent electrochemical experiments (see below).

2.3. Electrochemical experiments

2.3.1. Fabrication of the ITO-Au device

An ITO/Au modified glass slide was used as the working electrode. This electrode was obtained by sputtering a thin indium tin oxide (ITO) film (thickness 10 nm) followed by another film of gold (50 nm) onto a glass slide (Deckglaser Menzel-Glaser microscope cover slides, Fisher Scientific; 24 mm x 48 mm x 170 µm) using a sputtering system EMITECH K675X. ITO layer allowed good adhesion between glass and gold film. A PDMS (polydimethyloxane RTV-615; Momentive Performance Materials France) piece with a 9 mm diameter hole inside was attached on the ITO/Au modified glass slide by the mean of a treatment with oxygen plasma at 400 mtorr (100 W) for 3 min (Harrick Plasma, NY, USA). The final device thus corresponds to a PDMS well (volume ~0.5 ml) possessing the ITO/Au working electrode (9 mm in diameter) in the bottom. Appropriate electrical connections were made by using a copper wire and a silver paint (Radiospares) covered by an epoxy glue.

2.3.2. Cyclic voltammetry experiments

A platinum wire (30 x 1 mm) and a Ag/AgCl wire (35 x 0.5 mm) with chloride anions in solution (~8 mmol L^{-1}; see above) were used as counter and reference electrodes, respectively. Experiments were performed with aqueous solutions (500 µL) containing

quinones and/or algae within the gold PDMS well using a Parstat 2273 potentiostat (Princeton Applied Research). In the case of quinone/algae mixture, this corresponds to an excess of quinones since the mean ratio of photosystems and quinones is around 1:1000 (for instance with a concentration of algae equal to 2.10^7 cells mL^{-1} and a PSII concentration of 4.10^6 PSII $cells^{-1}$ [30] and a quinone concentration equal to 100 µmol L^{-1}). Actinic white light was provided by a Scott KL1500 LCD halogen lamp. The lamp was switched on 30 min before shutter opening to allow temperature stabilization. Once algae were incubated with quinones, the suspension was left in the well at open circuit voltage (OCV) for 5 seconds before launching the measurement. All the measurements with/without algae were carried out with constant scan rate ranging from 1 $mV.s^{-1}$ to 100 mV s^{-1} (5 kHz filter).

2.3.3. Photocurrent recording

The same set-up was used for chronoamperometry measurements. Quinones were added to the algae suspension and kept 5 seconds at OCV for equilibration. Then the working electrode was polarized at 0.38 V vs Ag/AgCl. After stabilization of the baseline, the light source shutter was opened, a faradic photocurrent being instantly generated. Light is turned off two minutes before the end of the experiment to allow the current to reach the baseline. All plots and statistical analyses (average values ± s.e.m.) were performed using SIGMA Plot 9.0 software (Systat Software Inc., Richmond, CA, USA).

3. Results and discussion

3.1.1. Validation of the miniaturized device

Chronoamperometry measurements were carried out using the well device containing algae suspension with 2,6-dichlorobenzoquinone (see experimental section). The electrode potential was appropriate to oxidize the hydroquinone ($QH_2 = Q + 2e^- + 2H^+$) resulting from the electron harvesting by the quinone form (**Figure 2A**). The background current observed after electrode polarization canceled after 90 s. This current magnitude decay (too long for a pure capacitive effect) may be ascribed to the faradaic re-oxidation of the fraction of hydroquinones generated by the algae metabolism in the presence of quinones under dark conditions.[24, 25, 27] Of note, the baseline current remained stable beyond this equilibration time (**Figure 2B**). As a consequence, the miniaturization of the electrode enhanced noticeably

the time response compared to the previously described setup with a carbon gauze electrode (a few minutes vs one hour respectively) according to a smaller electrode surface area in the new device. The illumination of algae in the medium supplemented with quinones triggered an instant photocurrent generation (**Figure 2B**) that directly results from the photosynthetic electron diverting from algae (see control experiments without algae or quinones in **Figure S1**). As expected, this photocurrent increased until reaching a steady state value. For given experimental conditions (quinone concentration, light illumination, algae concentration), reproducibility is quite good and is likely related to cell variability. For instance, chronoamperometry measurements (**Figure 2B**) from a suspension (2.10^7 cells mL^{-1}) illuminated at P = 60 mW cm^{-2} in presence of 2,6-DCBQ (100 µmol L^{-1}) gives a maximum current value (I_{max}) equal to (22.3 ± 3.9) µA. Photocurrents appeared sensitive to many experimental parameters (see below) and varied in the range of 10-30 µA, i.e. 16-50 µA cm^{-2}. These are common values for comparable biophotoelectrochemical systems. Subsequently, the lack of forced convection raised the question of the sedimentation of the algae suspension.

3.1.2. Algae sedimentaion did not affect photocurrent dynamics

A first way to evidence a possible sedimentation of the algae suspension during electron harvesting is to investigate the effect of the medium viscosity. Therefore, we performed chronoamperometry measurements with algae suspensions in minimum medium supplemented with Ficoll.[29] Indeed, Ficoll 400 is a high-mass (~ 400 kDa) and hydrophilic polysaccharide that is easily soluble in aqueous solution. It is known to hinder the cell motility without exceeding physiological osmolality and it was therefore used to prevent the suspension of sedimentation.[31] As displayed in **Figure 3A**, the recorded steady-state photocurrents with 2,6-DCBQ were lower in Ficoll supplemented medium ((22.3 ± 3.9) µA vs (13.8 ± 2.1) µA respectively. 2,6-DCBQ is an efficient electron acceptor so the same experiment was performed with 2,6-DMBQ whose ability to harvest electrons from the photosynthetic chain is rather moderate.[22, 24] The same trend was thus observed (**Figure S2**). The ratio of the photocurrents with and without Ficoll is about (1.6 ± 0.1) in both cases. This is globally consistent with the viscosity of a 10% w/v Ficoll solution (intrinsic viscosity being 17 cm^3 g^{-1}). Furthermore, normalized chronoamperograms (**Figure 3B** and **Figure S2**) demonstrate that the whole shape of the i = f(t) curve did not strongly depend on the medium as also evidenced by the half-time values (2,6-DCBQ : (135 ± 25) s with Ficoll vs (115 ± 15)

s without Ficoll; 2,6-DMBQ : (395 ± 40) s with Ficoll vs (350 ± 30) s without Ficoll). This suggests that sedimentation of the algae suspension did not significantly occur during electron diverting and that differences between the currents might be related to other parameters like quinones diffusion. Furthermore, this trend was confirmed by additional experiments where effects of natural and forced convection were investigated in presence of the reduced form of a dichloroquinone. Of note, this kind of experiments could not be achieved with dichloroquinone due to its ability to poison the biological system, as reported elsewhere.[25, 27] Thus two pre-treatments before applying the detection potential and light illumination were compared, i.e. with or without a pre-stirring of the algae suspension during 15 min (this delay globally corresponds to the transient phase of a representative chronoamperogram) before the electron harvesting. The corresponding chronoamperograms are displayed in **Figure 3C** and show that natural and forced convections before electron diverting had no significant effect (I_{max} = (19.8 ± 3.5) µA and $t_{1/2}$ = (20 ± 5) s without any previous stirring s vs I_{max} = (19.7 ± 3.0) s and $t_{1/2}$ = (15 ± 5) s after a pre-stirring; please note that half-times are faster in this case because the electrochemical oxidation of QH_2 near the electrode surface before illumination will lead to high local concentrations of quinones that increase extraction from algae.).

Therefore, these results show that the transient and steady-state phases are not significantly affected by sedimentation but are mainly due to the start of the diverting by the quinones (partitioning phenomena, electron harvesting along the chain and biological adjustment) before reaching a pseudo-equilibrium state between the extraction and oxidation reaction rates.

3.1.3. Cyclic voltammetry experiments

The device shown in **Figure 1B** was also used to perform cyclic voltammetry (CV) experiments on an algae suspension with 2,6-DCBQ (**Figure 4A**). Under dark conditions, the quasi-reversible CV of the QH_2/Q redox couple is observed as expected for a case where the electron harvesting by quinones did not take place. After illumination over 1 min, taking into account the faradic signals, the reduction peak ($Q \rightarrow QH_2$) decreases in favor of the oxidation peak ($QH_2 \rightarrow Q$). This shows the quite fast ability of quinones to accept electrons from the algae even when they are in such large excess and confirms the formation of the hydroquinone form during this reaction.

A way to investigate the process of current production is to consider cyclic voltammogramms of algae with hydroquinone species. CVs of algae suspension with dichlorohydroquinone are displayed in **Figure 4B**. At very low scan rates and under illumination (see also **Figure S3**), the electrogenerated quinones can interact with algae. The corresponding cyclic voltammogramm is only observed under light and is due to an electrocatalytic cycle involving two steps under illumination (QH_2 = Q + $2e^-$ + $2H^+$ and reduction of Q by the algae).

It is challenging to model in depth this system involving heterogeneous components (aqueous solution, algae, membranes, electrode…). First of all, the introduction of the electrochemical data collected from our quinone-algae system within a catalytic model developed for soluble species was not aimed at providing an accurate set of kinetic constants related to the photo-generation of QH_2. Our ambition here is to check whether the model provides turnover characteristics in keeping with the observation, thus allowing to use it for rough qualification of the performance of a given algae-quinone system. Therefore, several orders of magnitude can be extracted by means of some assumptions. In average, *Chlamydomonas reinhardtii* is a sphere of 3 µm radius.[32] Considering diffusion coefficients of quinones in aqueous solution (2.10^{-9} m^2 s^{-1}) and lipids (~ 10^{-16} m^2 s^{-1}),[33] the time for a quinone to cross a lipidic membrane (thicknesses ~ 4 nm) and aqueous compartments of an alga is around 180 ms. This is lower than the characteristic time (~ 5 s) deduced from the usual convection-diffusion thickness (100 µm). It therefore suggests that diffusion within algae can be neglected as a first approximation so the algae may be assimilated to uniform macrosystems catalyzing the reduction of exogenous quinones under illumination. As a consequence and because the quinone concentration is relatively low, electron harvesting may be roughly modeled as a pseudo-first order law (v = k'[Q]) by considering the excited site (PSII complex) concentration as a mean constant value. Combining these assumptions to the relatively low effect of sedimentation, the system may be globally considered as homogenenous and described as an electrocatalytical cycle where Q is reduced by algae to QH_2 and QH_2 is oxidized at the electrode surface to reform Q. Therefore, at low scan rates, the resulting S-shaped catalytic wave should be independent of scan rate according the following equation adapted to our experimental case: [34-36]

$$i = 2FS\frac{C^0_{QH_2}\sqrt{k'D_{QH_2}}}{1+\exp\left(-\frac{2F}{RT}(E-E°(QH_2/Q))\right)} \quad (1)$$

Where $C°_{QH2}$ is the added hydroquinone concentration, D_{QH2} is the diffusion coefficient of QH_2 and S is the electrode surface area.

For potential values higher than E°, the current remains constant according to :

$$i_{steady\ state} = 2FSC^0_{QH_2}\sqrt{k'D_{QH_2}} \quad (2)$$

In absence of substrate to reduce the electrogenerated Q, i.e. for a QH_2/algae mixture under dark conditions, the current follows the Randles-Sevcik's equation and depends on the scan rate "v" :

$$i^0_p = 0.446 \times 2FSC^0_{QH_2}\sqrt{\frac{2D_{QH_2}Fv}{RT}} \quad (3)$$

Finally, one obtains :

$$\frac{i_{steady\ state}}{i^0_p} = 2.24\sqrt{\frac{RT}{2Fv}k'} = 0.254\sqrt{\frac{k'}{v}} \quad (4)$$

This ratio directly depends on $v^{-1/2}$. However, it requires that the current plateau observed at 1 mV s^{-1} is the maximum value. Complementary amperometric measurements with the dichlorohydroquinone lead to a steady-state value "$i_{steady\ state}$" of 15.3 µA. This value will be coupled with the oxidation peaks "$i°_p$" from the CVs recorded as a function of the scan rate. The appropriate range of scan rates corresponding to an electrocatalytic behavior can be figured out by depicting the ratio of currents under illumination and dark conditions as a function of -log(v) (see **Figure S4**). Displaying $i_{steady\ state}/i°_p$ as a function of $v^{-1/2}$ results in a straight line shape (**Figure S5)**. The slope is equal to (0.163 ± 0.02) $V^{1/2}$ $s^{-1/2}$ and leads to k' = (0.41 ± 0.05) s^{-1}. In this view, k' is an apparent first order constant that takes into account the mean rate of electron harvesting among the reaction-diffusion layer. It is formally equal to the real rate constant multiplied by the substrate concentration (i.e. excited PSIIs) so it is actually related to the turnover frequency (TOF) of the catalyst. k' therefore accounts for the total number of excited PSIIs which will release their charge through the catalyst by unit of time. Of note, k' represents a global rate constant that encompasses all the electron extraction steps (including the quinone partitionning with membranes and cell compartements[22]). The corresponding half-time is therefore $t_{1/2}$ = ln2/k' ~ 1.7 s. In other words, 90 % of quinones are reduced after 6 s in accordance with the cyclic voltammograms mentioned above confirming an efficient catalysis. Furthermore, one can determine the diffusion-reaction layer according

to $\mu = (D/k')^{1/2} \sim 70$ µm. As expected, the current production is due to reactions occurring within a small equivalent volume of ~ 5 µL (i.e. 1 % of the volume of solution).

Of note, reducing this complicated biophotoelectrochemical system to a homogeneous electrocatalytical mechanism is an oversimplification. However, considering the timescales under study, this approximation finds its reliability in the fact that it gives access to interesting orders of magnitude to understand the phenomena involved in the electron diverting. Complementary views can be provided by investigating the effects of several experimental parameters.

3.2. Effects of experimental parameters

3.2.1. Quinone concentration

Photocurrents were recorded as a function of the concentrations of two exogenous quinones (2,6-DMBQ and 2,6-DCBQ) that behave differently in terms of their ability to harvest photosynthetic electrons from *Chlamydomonas reinhardtii* algae (2,6-DCBQ is significantly more efficient than 2,6-DMBQ).[22, 24] The curves are displayed in **Figure 5**. In both cases, the steady state current reaches a saturation point at high concentration. This is consistent with a Michaelis-Menten like behavior ($I_{ss} = I_{max}C_Q/(K_M+C_Q)$), as evidenced by the quite good correlations between the experimental and theoretical curves. This correlation is consistent with the ability of PSII to catalyze the reduction of exogenous quinones. Furthermore, this has been already demonstrated for other cases (isolated PSII, cyanobacteria…)[37-39] and confirms that the photocurrent production is globally controlled by the electron diverting by quinones.[25] In fact, at high concentrations, the extraction process is determined by the electron transfer itself and leads to a saturation of the current. Conversely, the harvesting is limited by the quinone arrival and leads to the current increase at low concentrations. Furthermore, the results obtained are consistent with the intrinsic capability of both quinones to interact with the photosynthetic chain (maximum steady-state value I_{max} = 44.5 and 14.8 µA; Michaelis constant K_M = 71.3 and 61.0 µmol.L^{-1} for 2,6-DCBQ and 2,6-DMBQ respectively).[22]

3.2.2. Algae concentration

Effects of algae concentration were also investigated. As displayed in **Figure 6**, the steady state photocurrents (recorded at t = 900 s) strongly depend on algae concentration. As expected, significant photocurrents were detected for high algae concentration in agreement with a larger number of available extraction sites within the suspension. However, a threshold is observed for algae concentrations of 8.10^7 cells mL^{-1}. In this case, oxygen may become scarce and consumption by algae becomes more difficult. It may therefore induce anaerobiosis that may limit the ability of the suspension to perform photosynthesis. It is worth mentioning that low quinones-algae ratios should disadvantage the electron diverting due to the ability of quinones to be sequestered in cell compartments before accessing the photosynthetic chain.[22]

Finally, considering time experiments over 1000 s demonstrated that the photocurrent progressively decreases at long timeframes (**Figure 6A**) according to a gradual poisoning of the suspension.[27]

3.2.3. Stability – day/night cycles

The progressive decrease occurring during the photocurrent production depends on the quinone concentration (**Figure 7A**). The photocurrent is especially stable for low added quinone concentrations (none or slow decrease after the maximum current for 2,6-DCBQ concentrations ranging from 50 to 100 µmol L^{-1}) in accordance with the poisoning effect of quinones that is concentration-dependent.[27] Conversely, higher 2,6-DCBQ concentrations lead to an immediate decrease after the maximum current value (slopes of $-(4.5 \pm 0.6)\ 10^{-3}$ µA s^{-1} and $-(8.3 \pm 1.2)\ 10^{-3}$ µA s^{-1} for 150 and 200 µmol L^{-1} respectively).

However, the stability of the electron harvesting process is also related to the illumination and induced photoinactivation phenomena. This can be featured by comparing experiments with a continuous illumination and day/night cycles. In the case of 2,6-DCBQ (**Figure 7B**), the decrease at long time frames is more significant for a continuous illumination, thus demonstrating that photoinactivation is also involved in the whole performance decrease of the electron harvesting. In the case of 2,6-DMBQ (**Figure S6**), the photocurrent reaches a steady state values under the same experimental conditions, as expected for this relatively low poisoning quinone.[27] Nevertheless, currents recorded by means of day/night cycles are still

higher than those measured under a continuous illumination. This shows again that photoinactivation occurs during the extraction. However, discriminating quinone poisoning and photoinactivation is not obvious. Indeed, electron harvesting mainly takes place within the diffusion-reaction layer, i.e. close to the electrode surface. Near the electrode surface and under illumination, the electrochemical oxidation of QH_2 leads to high local concentrations of quinones that both favor poisoning and extraction from algae. Under dark conditions, the electrogenerated quinones can diffuse out of the reaction layer limiting their possible toxic effect. The effect of quinones poisoning could only be investigated by recording chronoamperograms after a pre-incubation period (**Figure S7**). In the case of 2,6-DCBQ, the control experiment (no incubation) corresponds to the expected increase of current. Furthermore, the recorded currents at different incubation times gave better results at shorter times in accordance with the accumulation of quinones within the algae and the production of hydroquinones ready to be oxidized when applying light. Conversely, currents recorded at larger timeframes rapidly diminished because of the poisoning that occurred during the incubation. In all cases, this derivation appears to be harmful to the biological system whether by poisoning or photoinactivation. This result raises the question of the possible alleviation of the photosynthetic chain in the presence of exogenous quinones.

3.2.4. May quinones alleviate the photosynthetic chain?

Analyses involving this device confirmed that photoinactivation and quinone poisoning can occur during the extraction itself. However, this does not necessarily mean that electron diverting is not able to alleviate the photosynthetic chain under light illumination and prevent photoinactivation, this fact being a major concern for the stability of any bioelectrochemical photosynthetic system. This is why the previously described electrochemical experiments were also achieved with preliminary highly illuminated algae suspension. In this case, Δf1 mutants were considered because they lack b_6f complex.[40] The photosynthetic chain is therefore interrupted downstream of PSII complex making the algae more prone to undergo photoinactivation. As displayed in **Figure 8**, photocurrents with 2,6-DCBQ (one of the best PSII acceptors due its high redox potential [22]) are higher when no previous illumination was applied. It therefore suggests a protective effect at least at short times against photodamages and shows that the proper choice of quinone structure (as well as effective

diverting achieved by relevant concentrations) is necessary to achieve long-lasting experiments while also avoiding poisoning effects.

4. Conclusion

In this work, we reported on the use of a device involving a millimeter-sized gold electrode for investigating electron harvesting from a photosynthetic algae suspension. As long as no stirring wais applied, significant photocurrents were recorded. In this configuration, extraction was demonstrated to mainly occur near the electrode surface in a tiny reaction-diffusion layer, thus enabling to estimate a global extraction rate. Moreover, the relatively low surface area of the device helped to strongly decrease the equilibration time (once the potential was set at a value allowing the hydroquinone to be oxidized) compared to the previously reported set-up involving a centimeter sized carbon gauze. As a consequence, this device enabled us to perform larger number of experiments for investigating various effects of experimental parameters (quinone and algae concentrations, stability…). Because this analytical strategy confirmed some previous trends already observed at the preparative scale (poisoning, photoinactivation), it paves the way for setting future criteria toward the choice of quinone structure in order to attain maximum photocurrent stability over the long-term and performances for bioelectrochemical photosynthetic systems.

Acknowledgements

This work has been supported in part by CNRS (UMR 8640, UMR7141), Ecole Normale Supérieure, French Ministry of Research, Faculté des Sciences et Ingénierie - Sorbonne Université and the “Initiative d’Excellence” program from the French State (Grant “DYNAMO”, ANR-11-LABX-0011-01). G.L. and M.G.-C. thank Institut Universitaire de France Fellowship Program.

Figure 1

A)

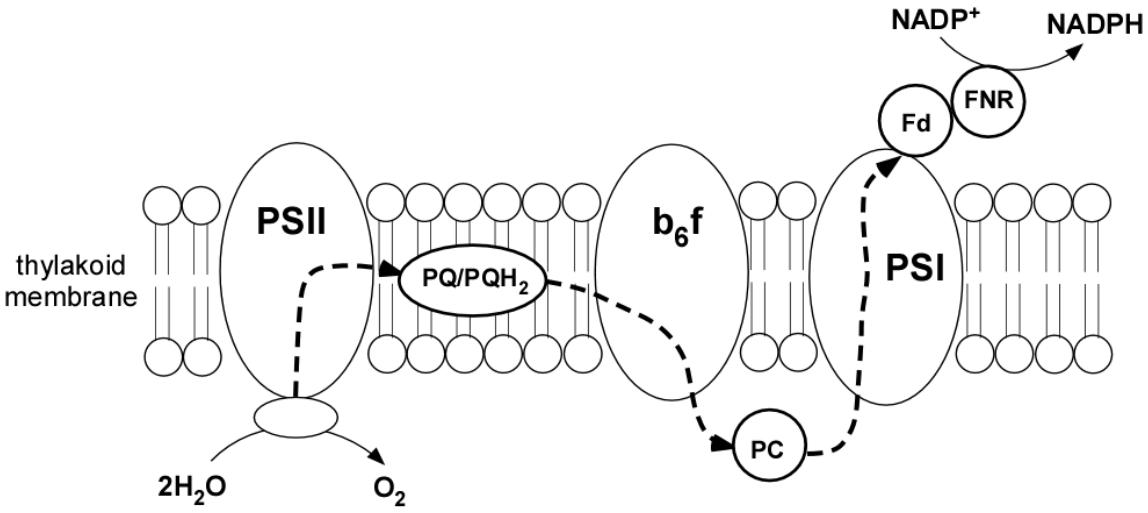
NADP+
NADPH
FNR
Fd
PSII
b6f
PSI
thylakoid membrane
PQ/PQH2
PC
2H2O
O2

B)

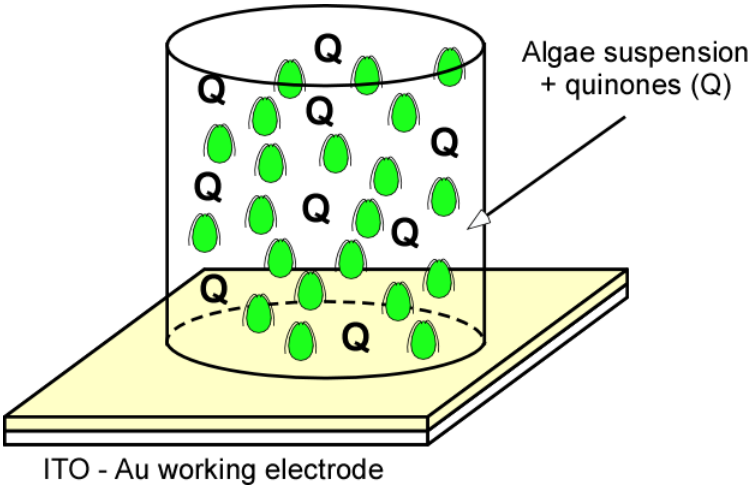
Q
Algae suspension
+ quinones (Q)
ITO - Au working electrode

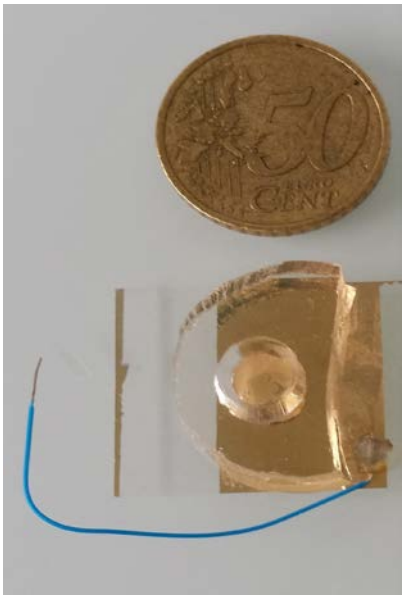

Figure 2

A)

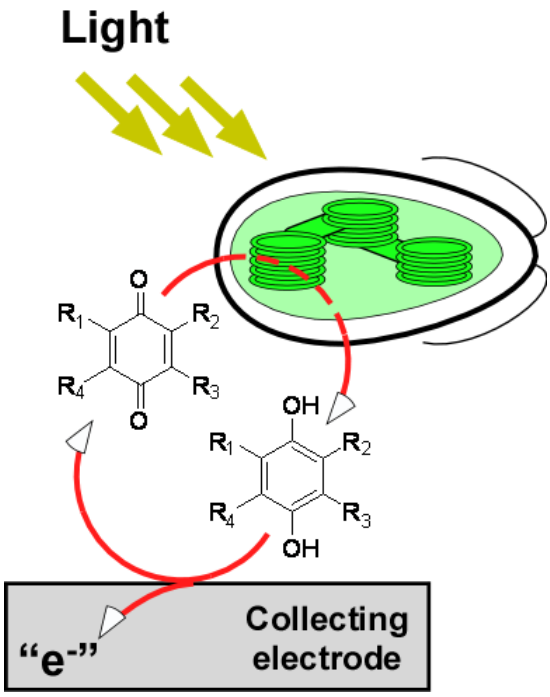
Light
O
R1
R2
R4
R3
O
OH
R1
R2
R4
R3
OH
"e-"
Collecting electrode

B)

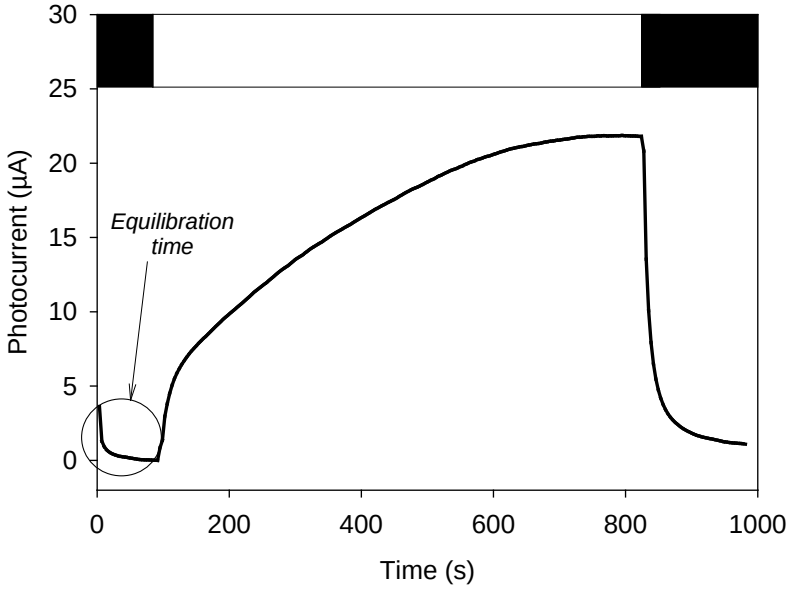
30
25
20
15
10
5
0
Photocurrent (µA)
Equilibration time
0
200
400
600
800
1000
Time (s)

Figure 3

A)

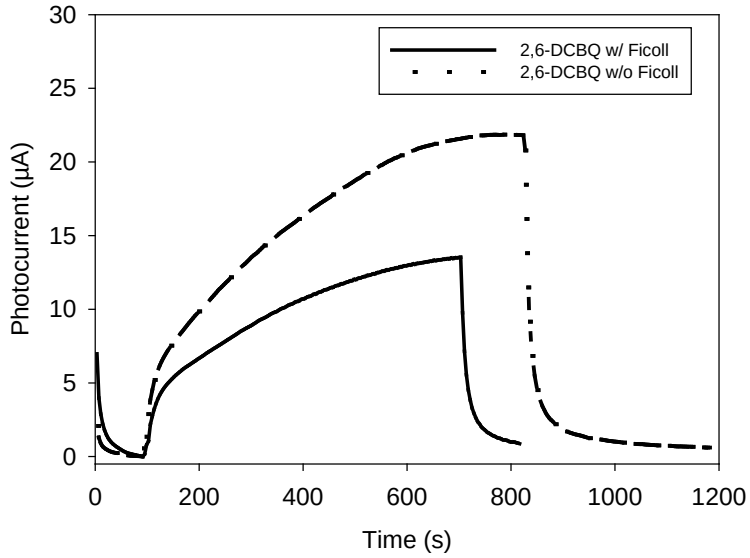
2,6-DCBQ w/ Ficoll
2,6-DCBQ w/o Ficoll
Photocurrent (μA)
Time (s)
0
5
10
15
20
25
30
0
200
400
600
800
1000
1200

B)

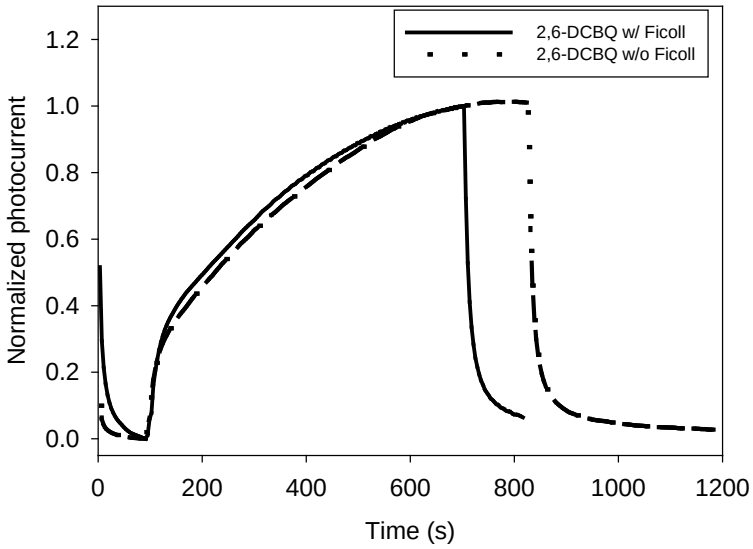
2,6-DCBQ w/ Ficoll
2,6-DCBQ w/o Ficoll
Normalized photocurrent
Time (s)
0.0
0.2
0.4
0.6
0.8
1.0
1.2
0
200
400
600
800
1000
1200

C)

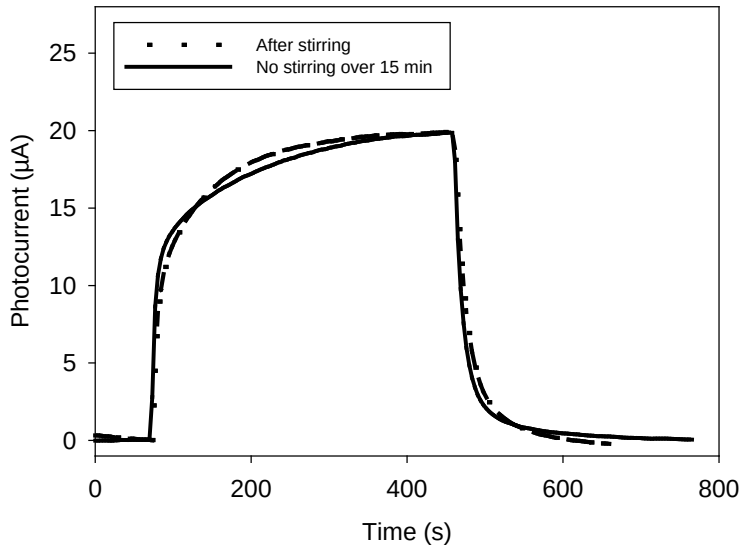
After stirring
No stirring over 15 min
Photocurrent (μA)
Time (s)
0
5
10
15
20
25
0
200
400
600
800

Figure 4

A)

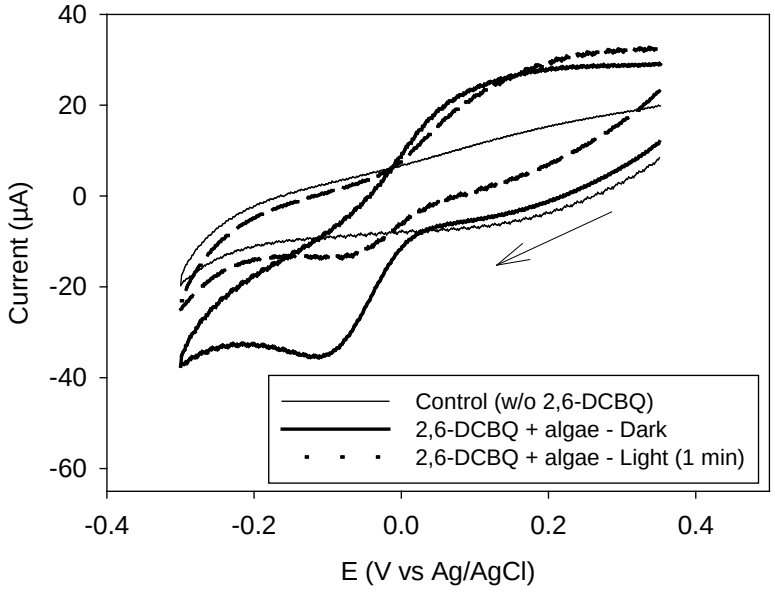
40
20
0
-20
-40
-60
Current (µA)
-0.4
-0.2
0.0
0.2
0.4
E (V vs Ag/AgCl)
Control (w/o 2,6-DCBQ)
2,6-DCBQ + algae - Dark
2,6-DCBQ + algae - Light (1 min)

B)

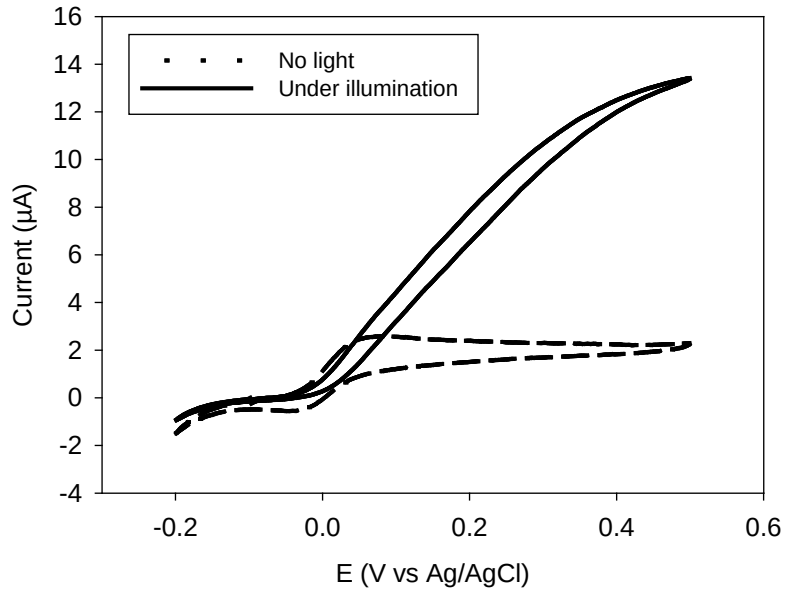
16
14
12
10
8
6
4
2
0
-2
-4
Current (µA)
-0.2
0.0
0.2
0.4
0.6
E (V vs Ag/AgCl)
No light
Under illumination

Figure 5

A)

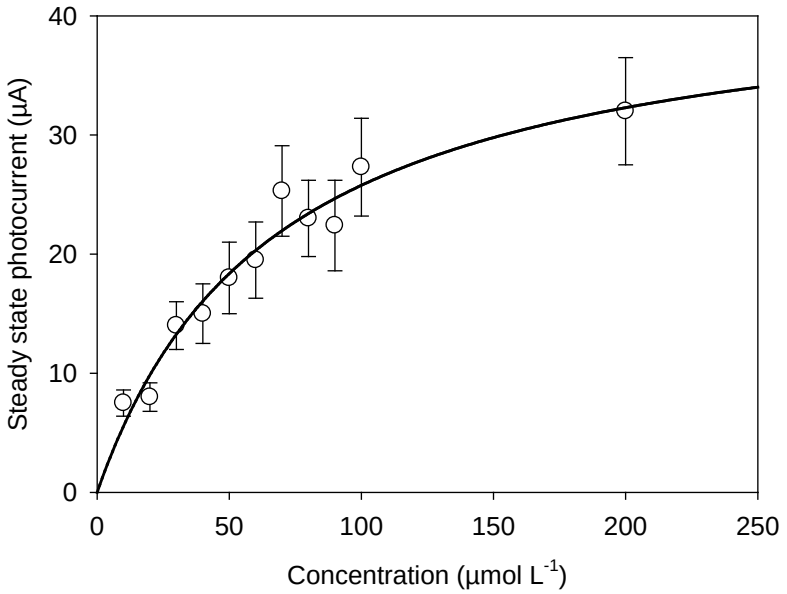
Steady state photocurrent (µA)
Concentration (µmol L-1)
0
10
20
30
40
0
50
100
150
200
250

B)

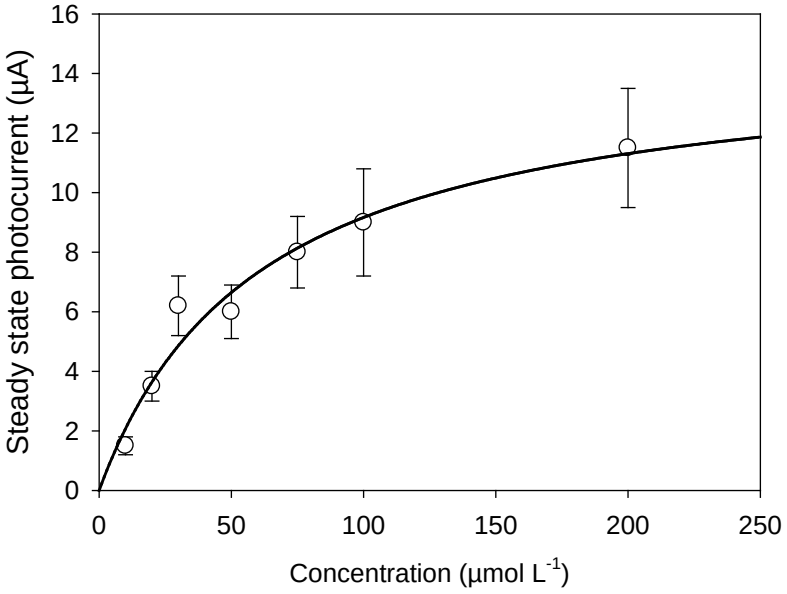
Steady state photocurrent (µA)
Concentration (µmol L-1)
0
2
4
6
8
10
12
14
16
0
50
100
150
200
250

Figure 6

A)

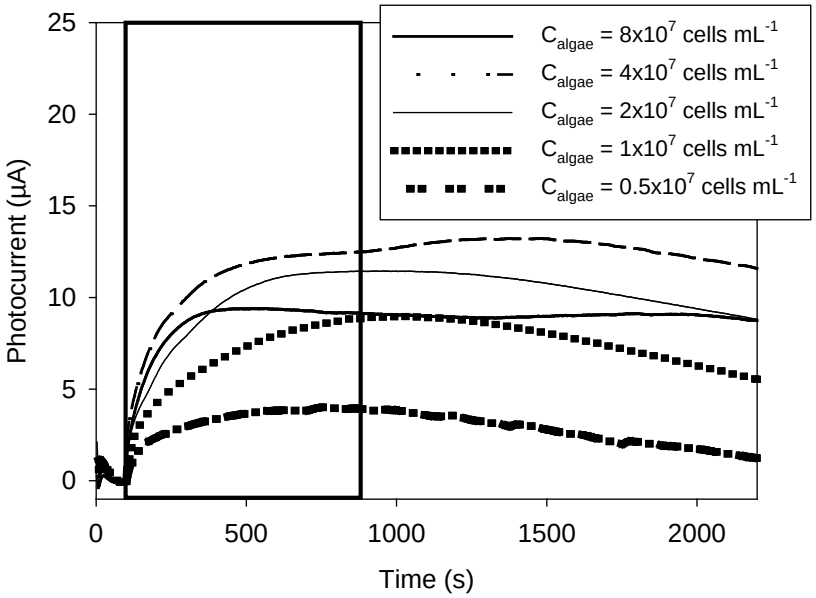
Photocurrent (µA)
Time (s)
0
5
10
15
20
25
0
500
1000
1500
2000
C_{algae} = 8x10^7 cells mL^{-1}
C_{algae} = 4x10^7 cells mL^{-1}
C_{algae} = 2x10^7 cells mL^{-1}
C_{algae} = 1x10^7 cells mL^{-1}
C_{algae} = 0.5x10^7 cells mL^{-1}

B)

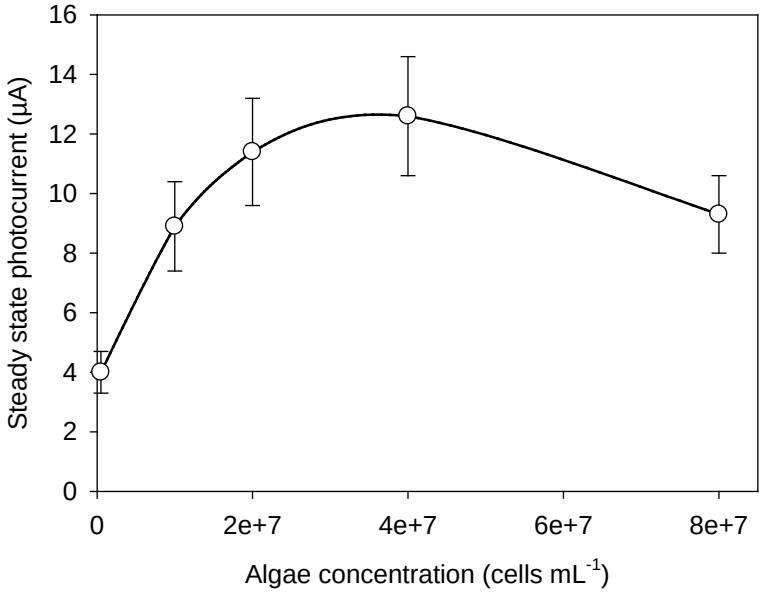
Steady state photocurrent (µA)
Algae concentration (cells mL^{-1})
0
2
4
6
8
10
12
14
16
0
2e+7
4e+7
6e+7
8e+7

Figure 7

A)

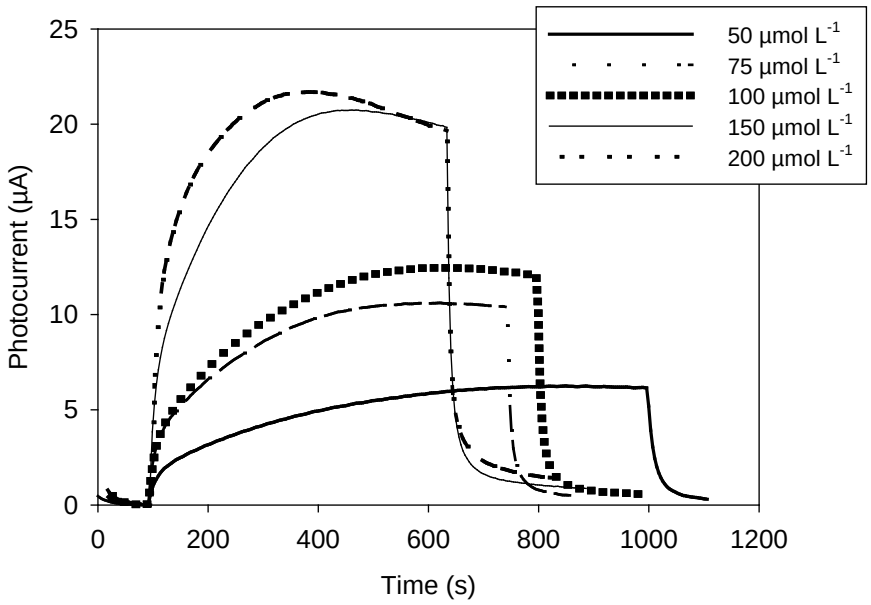
50 µmol L-1
75 µmol L-1
100 µmol L-1
150 µmol L-1
200 µmol L-1
Photocurrent (µA)
Time (s)
0
5
10
15
20
25
0
200
400
600
800
1000
1200

B)

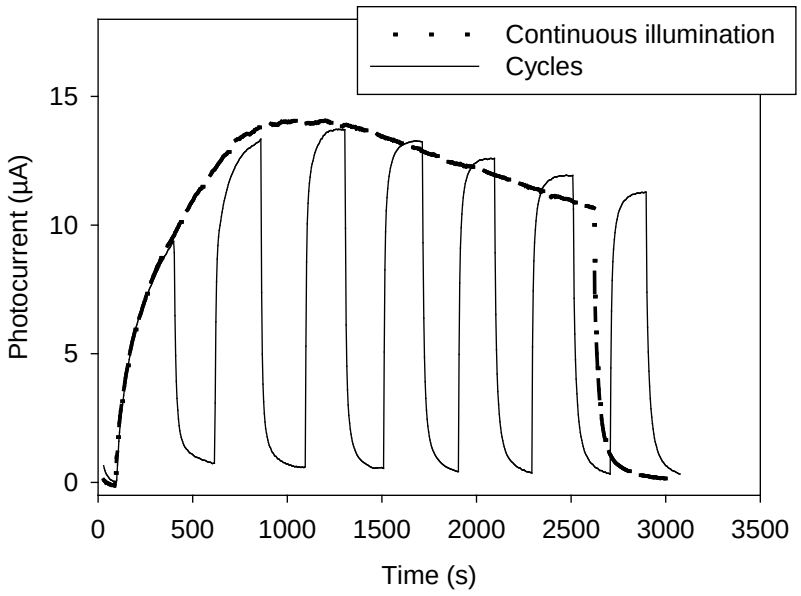
Continuous illumination
Cycles
Photocurrent (µA)
Time (s)
0
5
10
15
0
500
1000
1500
2000
2500
3000
3500

Figure 8

A)

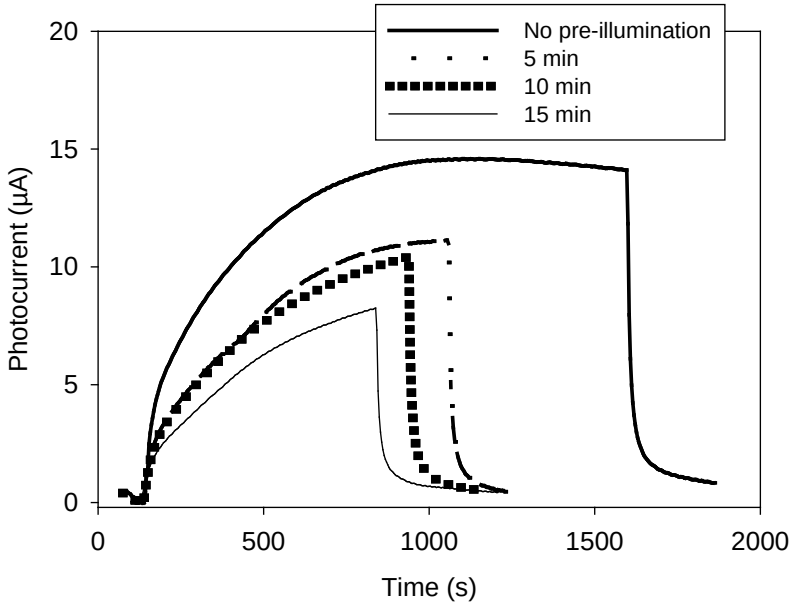
No pre-illumination
5 min
10 min
15 min
Photocurrent (µA)
Time (s)
0
5
10
15
20
0
500
1000
1500
2000

B)

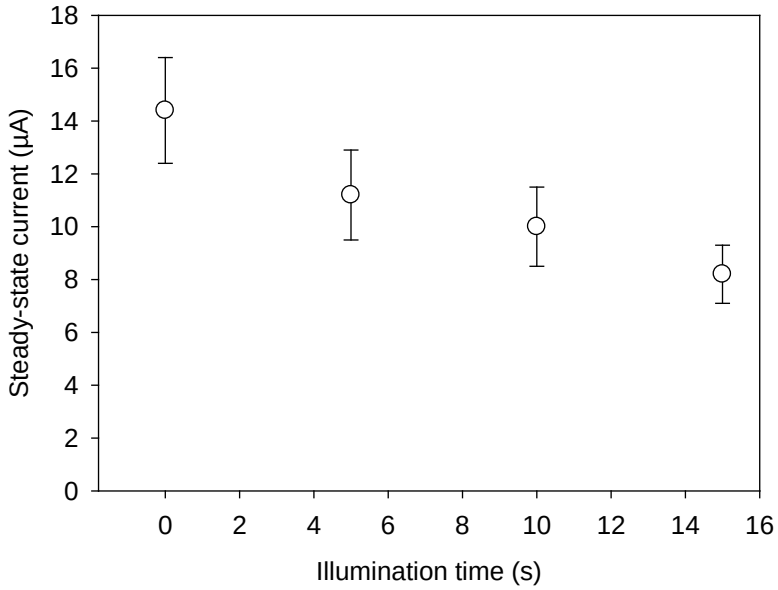
Steady-state current (µA)
Illumination time (s)
0
2
4
6
8
10
12
14
16
18

Figure captions

Figure 1. A) Scheme of the photosynthetic chain. B) Configuration of the electrochemical experiments involving an algae suspension in presence of quinones by means of the ITO-Au device. Left : scheme; Right : photograph.

Figure 2. A) Scheme of the electrocatalytical cycle inducing the production of a photocurrent from an algae suspension under light illumination in presence of exogenous quinones. The photosynthetic chain is embedded in the chloroplast and consists of thylakoid membranes and different complexes (see text). B) Representative chronoamperometric trace (E_W = 0.38 V vs Ag/AgCl) from a suspension of *Chlamydomonas reinhardtii* algae (2.10^7 cells mL^{-1}) with 2,6-DCBQ (100 µmol L^{-1}) under illumination (P = 60 mW cm^{-2}; white rectangle).

Figure 3. Chronoamperograms from a suspension of *Chlamydomonas reinhardtii* algae (2.10^7 cells mL^{-1}) under illumination (P = 60 mW cm^{-2}). A) Current = f(t) with 2,6-DCBQ (100 µmol L^{-1}) : with (solid line) and without (dashed line) Ficoll ; B) Normalized current = f(t) with 2,6-DCBQ (100 µmol L^{-1}) with (solid line) and without (dashed line) Ficoll. C) Current = f(t) with 2,5-DCHQ (100 µmol L^{-1}) with (dashed line) or without (solid line) any pre-stirring. Please note that 2,6-DCHQ is not commercially supplied. Because 2,6-DCBQ and 2,5-DCBQ have a similar behavior,[22, 27] the commercially available 2,5-DCHQ is used in this peculiar experiment (see text).

Figure 4. Cyclic voltammograms of a suspension of *Chlamydomonas reinhardtii* (2.10^7 cells mL^{-1}). A) With 2,6-DCBQ (100 µmol L^{-1}) : under dark conditions (solid line) or under illumination (dashed line; 60 mW cm^{-2}) over 1 min. v = 100 mV s^{-1} B) With 2,5-DCHQ (100 µmol L^{-1}) : under dark conditions (dashed line) or under illumination (solid line; 60 mW cm^{-2}). v = 1 mV s^{-1}.

Figure 5. Steady state photocurrents recorded with a suspension of *Chlamydomonas reinhardtii* algae (2.10^7 cells mL^{-1}) under illumination (P = 60 mW cm^{-2}) as a function of added quinone concentration for two exogenous quinones : A) 2,6-DCBQ ; B) 2,6-DMBQ. The experimental curves were modeled by means of a Michael-Menten like behavior ($Iss = AC_Q/(B+C_Q)$; R^2 = 0.97).

Figure 6. A) Chronoamperograms from several suspensions of *Chlamydomonas reinhardtii* algae under illumination (P = 60 mW cm^{-2}) with 2,6-DCBQ (100 µmol L^{-1}). The rectangle

shows the timeframe where the current increased until reaching a steady state value. B) Steady state current (t = 900 s) as a function of algae concentration.

Figure 7. A) Chronoamperograms from a suspension of *Chlamydomonas reinhardtii* algae (2.10^7 cells mL^{-1}) under illumination (P = 20 mW cm^{-2}) with different 2,6-DCBQ concentrations (50-200 µmol L^{-1}). B) Chronoamperograms from a suspension of *Chlamydomonas reinhardtii* algae under the same conditions with 2,6-DCBQ (100 µmol L^{-1}) : solid line : day/night cycles ; dashed line : continuous illumination.

Figure 8. A) Chronoamperograms from a suspension of *Chlamydomonas reinhardtii* algae (Δf1) under illumination (P = 60 mW cm^{-2}) with 2,6-DCBQ (100 µmol L^{-1}) after different times of pre-illumination. B) Steady state photocurrents recorded as a function of the pre-illumination time.

References

[1] R.E. Blankenship, D.M. Tiede, J. Barber, G.W. Brudvig, G. Fleming, M. Ghirardi, M.R. Gunner, W. Junge, D.M. Kramer, A. Melis, T.A. Moore, C.C. Moser, D.G. Nocera, A.J. Nozik, D.R. Ort, W.W. Parson, R.C. Prince, R.T. Sayre, Comparing Photosynthetic and Photovoltaic Efficiencies and Recognizing the Potential for Improvement, Science, 332 (2011) 805-809.

[2] N. Sekar, R.P. Ramasamy, Recent advances in photosynthetic energy conversion, J. Photochem. Photobiol. C, 22 (2015) 19-33.

[3] R.A. Voloshin, V.D. Kreslavski, S.K. Zharmukhamedov, V.S. Bedbenov, S. Ramakrishna, S.I. Allakhverdiev, Photoelectrochemical cells based on photosynthetic systems: a review, Biofuel Res. J., 2 (2015) 227-235.

[4] A.J. McCormick, P. Bombelli, R.W. Bradley, R. Thorne, T. Wenzel, C.J. Howe, Biophotovoltaics: oxygenic photosynthetic organisms in the world of bioelectrochemical systems, Energy Environ. Sci., 8 (2015) 1092-1109.

[5] A. Badura, T. Kothe, W. Schuhmann, M. Roegner, Wiring photosynthetic enzymes to electrodes, Energy Environ. Sci., 4 (2011) 3263-3274.

[6] M. Kato, J.Z. Zhang, N. Paul, E. Reisner, Protein film photoelectrochemistry of the water oxidation enzyme photosystem II, Chem. Soc. Rev., 43 (2014) 6485-6497.

[7] R. Tel-Vered, I. Willner, Photo-bioelectrochemical Cells for Energy Conversion, Sensing, and Optoelectronic Applications, ChemElectroChem, 1 (2014) 1778-1797.

[8] J.O. Calkins, Y. Umasankar, H. O'Neill, R.P. Ramasamy, High photo-electrochemical activity of thylakoid-carbon nanotube composites for photosynthetic energy conversion, Energy Environ. Sci., 6 (2013) 1891-1900.

[9] K. Hasan, Y. Dilgin, S.C. Emek, M. Tavahodi, H.-E. Akerlund, P.-A. Albertsson, L. Gorton, Photoelectrochemical Communication between Thylakoid Membranes and Gold Electrodes through Different Quinone Derivatives, ChemElectroChem, 1 (2014) 131-139.

[10] K. Hasan, R.D. Milton, M. Grattieri, T. Wang, M. Stephanz, S.D. Minteer, Photobioelectrocatalysis of Intact Chloroplasts for Solar Energy Conversion, ACS Catal., 7 (2017) 2257-2265.

[11] R.I. Pinhassi, D. Kallmann, G. Soper, S. Larom, A. Linkov, A. Boulouis, M.A. Schottler, R. Bock, A. Rothschild, N. Adir, G. Schuster, Photosynthetic Membranes of Synechocystis or Plants Convert Sunlight to Photocurrent through Different Pathways due to Different Architectures, Plos One, 10 (2015) e0122616.

[12] M. Rasmussen, A. Shrier, S.D. Minteer, High performance thylakoid bio-solar cell using laccase enzymatic biocathodes, Phys. Chem. Chem. Phys., 15 (2013) 9062-9065.
[13] K. Hasan, V. Grippo, E. Sperling, M.A. Packer, D. Leech, L. Gorton, Evaluation of Photocurrent Generation from Different Photosynthetic Organisms, ChemElectroChem, 4 (2017) 412-417.
[14] N. Sekar, Y. Umasankar, R.P. Ramasamy, Photocurrent generation by immobilized cyanobacteria via direct electron transport in photo-bioelectrochemical cells, Phys. Chem. Chem. Phys., 16 (2014) 7862-7871.
[15] M. Grattieri, K. Hasan, S.D. Minteer, Bioelectrochemical Systems as a Multipurpose Biosensing Tool: Present Perspective and Future Outlook, ChemElectroChem, 4 (2017) 834-842.
[16] J.A. Laureanti, A.K. Jones, Photosynthetic Microbial Fuel Cells, Adv. Biochem. Engin./Biotechnol., 158 (2016) 159-175.
[17] D.P.B.T.B. Strik, R.A. Timmers, M. Helder, K.J.J. Steinbusch, H.V.M. Hamelers, C.J.N. Buisman, Microbial solar cells: applying photosynthetic and electrochemically active organisms, Trends Biotechnol., 29 (2011) 41-49.
[18] J.Z. Zhang, P. Bombelli, K.P. Sokol, A. Fantuzzi, A.W. Rutherford, C.J. Howe, E. Reisner, Photoelectrochemistry of Photosystem II &ITin Vitro&IT vs&IT in Vivo&IT, J. Am. Chem. Soc., 140 (2018) 6-9.
[19] L.H. Kim, Y.J. Kim, H. Hong, D. Yang, M. Han, G. Yoo, H.W. Song, Y. Chae, J.-C. Pyun, A.R. Grossman, W. Ryu, Patterned Nanowire Electrode Array for Direct Extraction of Photosynthetic Electrons from Multiple Living Algal Cells, Adv. Funct. Mater., 26 (2016) 7679-7689.
[20] W. Ryu, S.-J. Bai, J.S. Park, Z. Huang, J. Moseley, T. Fabian, R.J. Fasching, A.R. Grossman, F.B. Prinz, Direct Extraction of Photosynthetic Electrons from Single Algal Cells by Nanoprobing System, Nano Lett., 10 (2010) 1137-1143.
[21] Y.J. Kim, J. Yun, S.I. Kim, H. Hong, J.-H. Park, J.-C. Pyun, W. Ryu, Scalable long-term extraction of photosynthetic electrons by simple sandwiching of nanoelectrode array with densely-packed algal cell film, Biosens. Bioelectron., 117 (2018) 15-22.
[22] G. Longatte, H.Y. Fu, O. Buriez, E. Labbe, F.A. Wollman, C. Amatore, F. Rappaport, M. Guille-Collignon, F. Lemaître, Evaluation of photosynthetic electrons derivation by exogenous redox mediators, Biophys. Chem., 205 (2015) 1-8.

[23] G. Longatte, F. Rappaport, F.A. Wollman, M. Guille-Collignon, F. Lemaître, Mechanism and analyses for extracting photosynthetic electrons using exogenous quinones - what makes a good extraction pathway?, Photochem. Photobiol. Sci., 15 (2016) 969-979.
[24] H.Y. Fu, D. Picot, Y. Choquet, G. Longatte, A. Sayegh, J. Delacotte, M. Guille-Collignon, F. Lemaître, F. Rappaport, F.A. Wollman, Redesigning the Q(A) binding site of Photosystem II allows reduction of exogenous quinones, Nature Commun., 8 (2017) 15274.
[25] G. Longatte, F. Rappaport, F.A. Wollman, M. Guille-Collignon, F. Lemaître, Electrochemical Harvesting of Photosynthetic Electrons from Unicellular Algae Population at the Preparative Scale by Using 2,6-dichlorobenzoquinone, Electrochim. Acta, 236 (2017) 327-332.
[26] G. Longatte, M. Guille-Collignon, F. Lemaître, Electrocatalytic Mechanism Involving Michaelis-Menten Kinetics at the Preparative Scale: Theory and Applicability to Photocurrents from a Photosynthetic Algae Suspension With Quinones, ChemPhysChem, 18 (2017) 2643-2650.
[27] G. Longatte, A. Sayegh, J. Delacotte, F. Rappaport, F.-A. Wollman, M. Guille-Collignon, F. Lemaître, Investigation of photocurrents resulting from a living unicellular algae suspension with quinones over time, Chem. Sci., 9 (2018) 8271-8281.
[28] M. Grattieri, Z. Rhodes, D.P. Hickey, K. Beaver, S.D. Minteer, Understanding Biophotocurrent Generation in Photosynthetic Purple Bacteria, ACS Catal., 9 (2019) 867-873.
[29] W.J. Nawrocki, S. Santabarbara, L. Mosebach, F.-A. Wollman, F. Rappaport, State transitions redistribute rather than dissipate energy between the two photosystems in Chlamydomonas, Nature Plants, 2 (2016) 16031.
[30] H. Kirst, J.G. Garcia-Cerdan, A. Zurbriggen, T. Ruehle, A. Melis, Truncated Photosystem Chlorophyll Antenna Size in the Green Microalga Chlamydomonas reinhardtii upon Deletion of the TLA3-CpSRP43 Gene, Plant Physiol., 160 (2012) 2251-2260.
[31] B. Qin, A. Gopinath, J. Yang, J.P. Gollub, P.E. Arratia, Flagellar Kinematics and Swimming of Algal Cells in Viscoelastic Fluids, Sci. Rep., 5 (2015) 9190.
[32] R.A. Craigie, T. Cavaliersmith, CELL-VOLUME AND THE CONTROL OF THE CHLAMYDOMONAS CELL-CYCLE, J. Cell Sci., 54 (1982) 173-191.
[33] A. Ilani, T. Krakover, DIFFUSION-LIMITED AND REACTION RATE-LIMITED REDOX PROCESSES MEDIATED BY QUINONES THROUGH BILAYER LIPID-MEMBRANES, Biophys. J., 51 (1987) 161-167.
[34] H.H. Girault, Analytical and Physical Electrochemistry, EPFL Press, 2004.

[35] C. Costentin, S. Drouet, M. Robert, J.-M. Saveant, Turnover Numbers, Turnover Frequencies, and Overpotential in Molecular Catalysis of Electrochemical Reactions. Cyclic Voltammetry and Preparative-Scale Electrolysis, J. Am. Chem. Soc., 134 (2012) 11235-11242.
[36] C. Costentin, S. Drouet, M. Robert, J.-M. Saveant, Turnover Numbers, Turnover Frequencies, and Overpotential in Molecular Catalysis of Electrochemical Reactions. Cyclic Voltammetry and Preparative-Scale Electrolysis (vol 134, pg no 11235, 2012), J. Am. Chem. Soc., 134 (2012) 19949-19950.
[37] M. Kasuno, M. Torimura, Y. Tsukatani, D. Murakami, S. Hanada, T. Matsushita, H. Tao, Characterization of the photoinduced electron transfer reaction from the photosynthetic system in Rhodobacter sphaeroides to an exogenous electron acceptor, J. Electroanal. Chem., 636 (2009) 101-106.
[38] M. Torimura, A. Miki, A. Wadano, K. Kano, T. Ikeda, Electrochemical investigation of cyanobacteria Synechococcus sp PCC7942-catalyzed photoreduction of exogenous quinones and photoelectrochemical oxidation of water, J. Electroanal. Chem., 496 (2001) 21-28.
[39] K. Brinkert, F. Le Formal, X. Li, J. Durrant, A.W. Rutherford, A. Fantuzzi, Photocurrents from photosystem II in a metal oxide hybrid system: Electron transfer pathways, Biochim Biophys Acta Bioenerg., 1857 (2016) 1497-1505.
[40] B. Rimbault, D. Esposito, D. Drapier, Y. Choquet, D. Stern, F.A. Wollman, Identification of the initiation codon for the atpB gene in Chlamydomonas chloroplasts excludes translation of a precursor form of the beta subunit of the ATP synthase, Mol. Gen. Genet., 264 (2000) 486-491.

Supporting Information

Diverting Photosynthetic Electrons from Suspensions of *Chlamydomonas reinhardtii* Algae - New Insights using an Electrochemical Well Device

Adnan Sayegh, Guillaume Longatte, Olivier Buriez, Francis-André Wollman, Manon Guille-Collignon, Eric Labbé, Jérôme Delacotte, Frédéric Lemaître

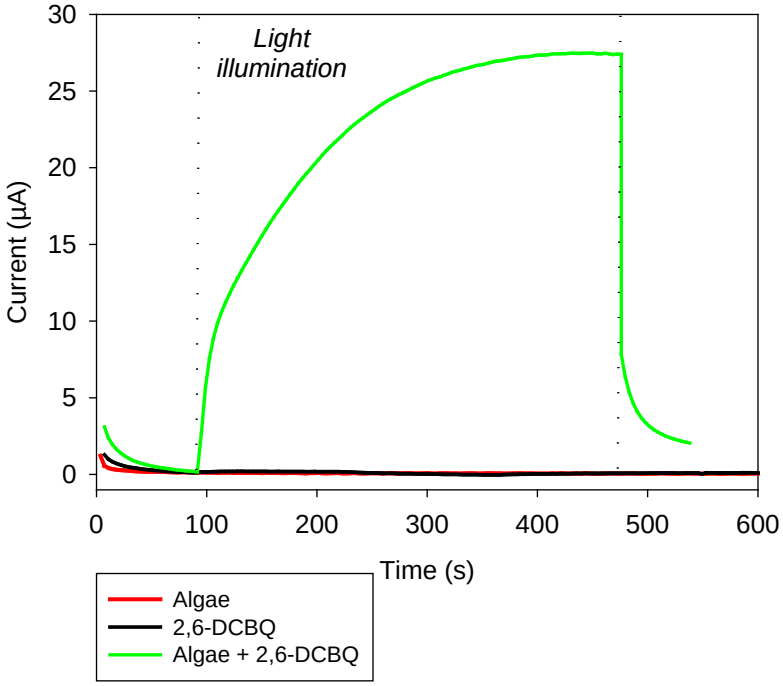

Figure S1. Chronoamperograms (E_W = 0.38 V vs Ag/AgCl) using the Au-ITO device under illumination (P = 60 mW cm^{-2}). Green line : from a suspension of *Chlamydomonas reinhardtii* algae (2.10^7 cells mL^{-1}) with 2,6-DCBQ (100 µmol L^{-1}) ; black line : 2,6-DCBQ (100 µmol L^{-1}) alone ; red line : only a suspension of *Chlamydomonas reinhardtii* algae (2.10^7 cells mL^{-1}).

A)

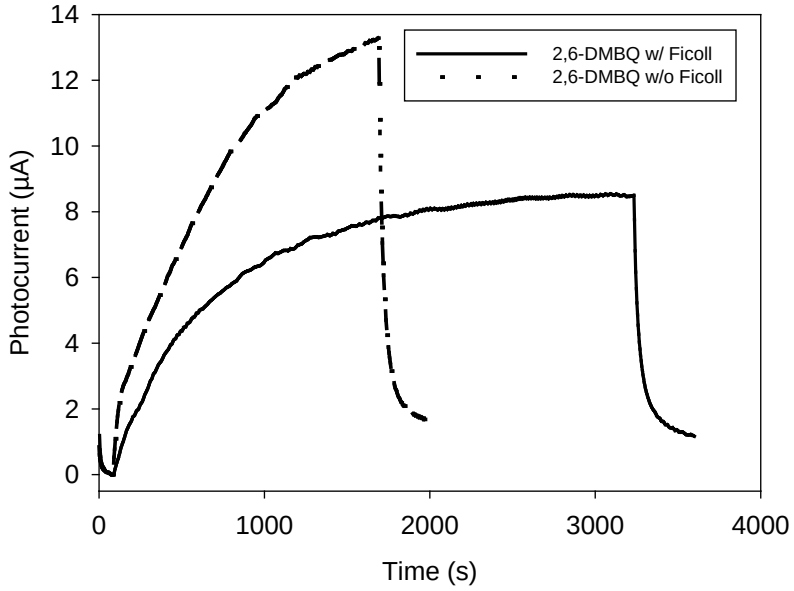

B)

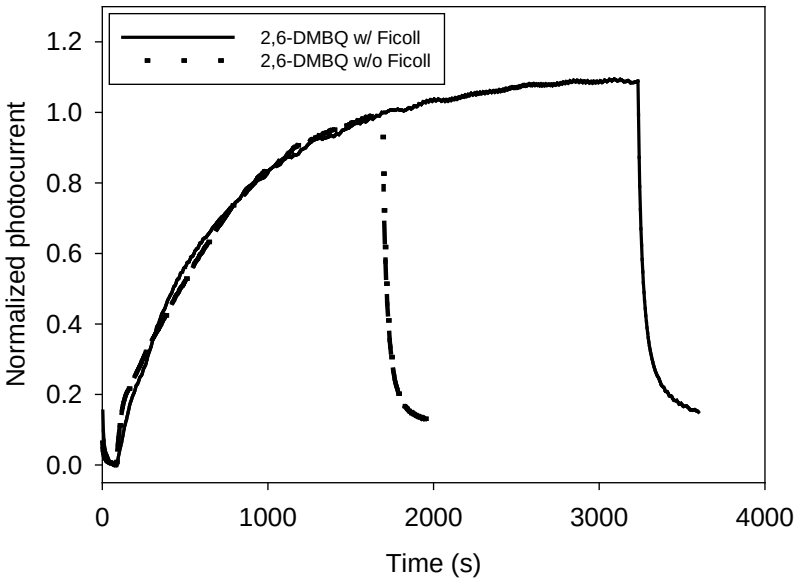

Figure S2. Chronoamperograms (E_W = 0.38 V vs Ag/AgCl) from a suspension of *Chlamydomonas reinhardtii* algae (2.10^7 cells mL^{-1}) under illumination (P = 60 mW cm^{-2}). A) Current = f(t) with 2,6-DMBQ (100 µmol L^{-1}) ; B) Normalized current = f(t) with 2,6-DMBQ (100 µmol L^{-1}).

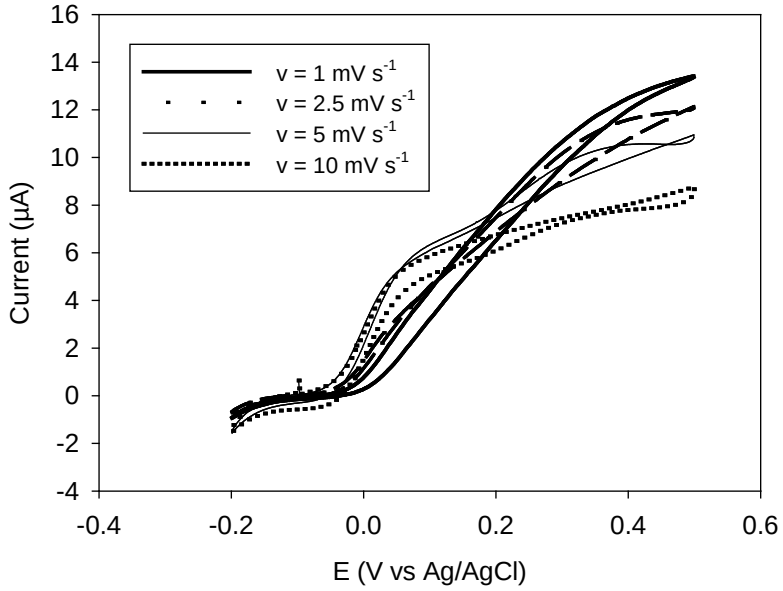

Figure S3. Cyclic voltammograms of a suspension of *Chlamydomonas reinhardtii* (2.10^7 cells mL^{-1}) with 2,5-DCHQ (100 µmol L^{-1}) under illumination (solid line; 60 mW cm^{-2}) at different scan rates (1; 2.5; 5 and 10) mV s^{-1}.

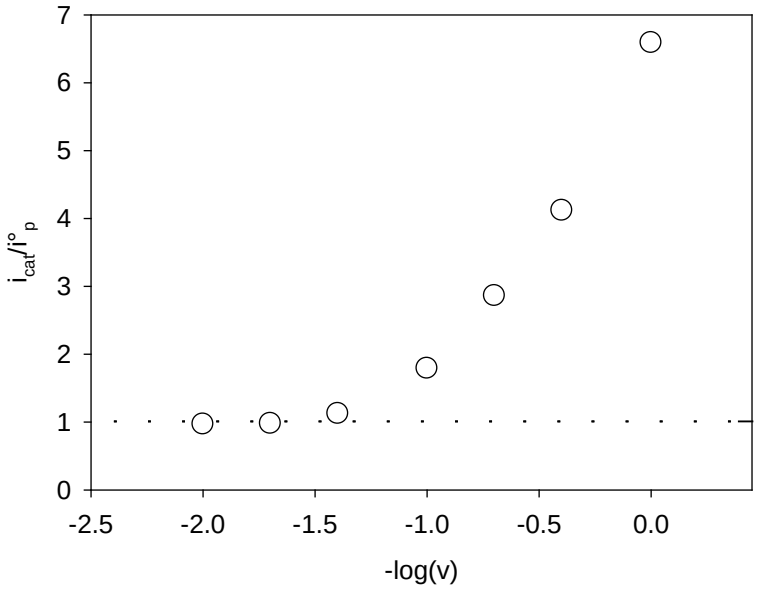

Figure S4. Ratio of currents under illumination (60 mW cm^{-2} ; i_{cat}) and under dark conditions ($i°_p$) as a function of the scan rate for a suspension of *Chlamydomonas reinhardtii* (2.10^7 cells mL^{-1}) with 2,5-DCHQ (100 µmol L^{-1}).

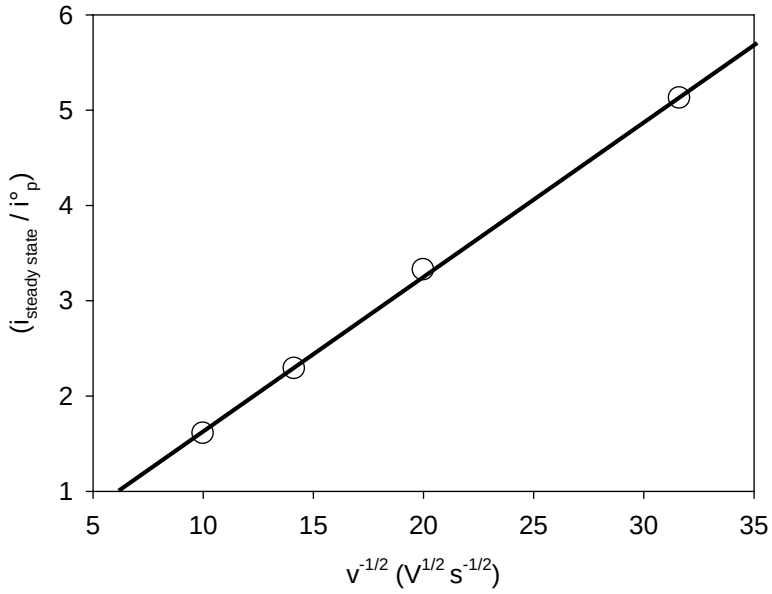

Figure S5. Ratio of the steady state current under illumination (15.3 µA; 60 mW cm^{-2}) and the current peak under dark conditions ($i°_p$) as a function of $v^{-1/2}$ for a suspension of *Chlamydomonas reinhardtii* (2.10^7 cells mL^{-1}) with 2,5-DCHQ (100 µmol L^{-1}).

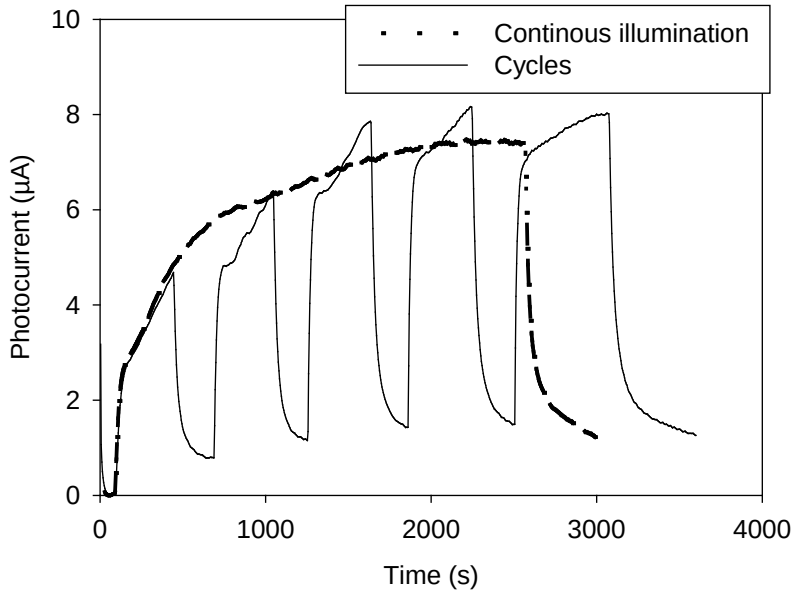

Figure S6. Chronoamperograms from a suspension of *Chlamydomonas reinhardtii* algae (2.10^7 cells mL^{-1}) under illumination (P = 60 mW cm^{-2}) with 2,6-DMBQ (100 µmol L^{-1}). Solid line : day/night cycles ; dashed line : continuous illumination.

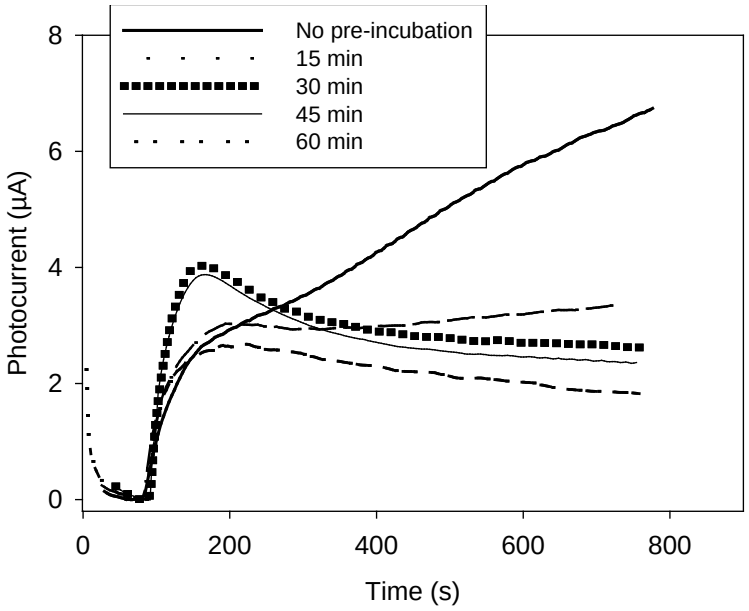

Figure S7. Chronoamperograms from a suspension of *Chlamydomonas reinhardtii* algae (2.10^7 cells mL^{-1}) under illumination (P = 60 mW cm^{-2}). 2,6-DCBQ (100 µmol L^{-1}) is incubated at different times before triggering light illumination.